PCCP

Accepted Manuscript

ROYAL SOCIETY OF CHEMISTRY

www.rsc.org/pccp

A graphical and textual abstract for the Table of contents entry

Size-selected Pt_n clusters on the Al_2O_3 surface form two-dimensional planar structures at $n \leq 18$ and three-dimensional two-layer structures start to appear at $n \geq 19$. They are composed of neutral and cationic Pt atoms.

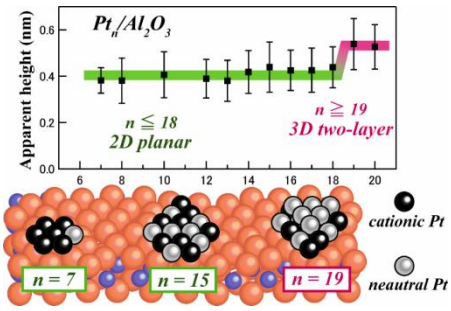

Morphology and chemical states of size-selected Pt_n clusters on an aluminium oxide film on NiAl(110)

Atsushi Beniya[a], Noritake Isomura[a], Hirohito Hirata[b] and Yoshihide Watanabe[a,*]

Abstract

The adsorption states of size-selected Pt_n clusters ($7 \leq n \leq 20$) soft-landed on an Al_2O_3/NiAl(110) substrate were investigated using scanning tunneling microscopy, infrared reflection absorption spectroscopy, and temperature programmed desorption. Pt_n clusters lay flat on the surface with a planar structure ($n \leq 18$), and three-dimensional two-layer clusters start to appear at $n \geq 19$. By considering the Pt-Pt and Pt-oxide bonds in the cluster, the morphological transition could be reasonably explained. Using CO probe molecules, the chemical states of the Pt atoms inside the clusters were investigated. Two ontop CO species were observed inside the clusters, and were assigned as adsorbed CO on neutral and slightly cationic Pt atoms. Despite of the first layer Pt atoms, the Pt_n clusters are composed of the two kinds of Pt atoms. The observed size dependence of the Pt atoms inside the clusters may contribute to the size-dependent chemical reactivity of Pt_n clusters on the Al_2O_3 surface.

Keywords

Size-selected cluster, Soft-landing, Scanning tunneling microscopy, Infrared reflection absorption spectroscopy, Temperature programmed desorption, Al_2O_3, Pt, CO

1. Introduction

Size-selected atomic clusters on surfaces are a subject of considerable interest because of their distinctive size-dependent catalytic properties.[1,2] Catalytic activity and efficiency will depend on the size, composition, morphology, and electronic state of both the metal clusters and the supports. Metal clusters supported on oxide substrates serve as model systems for investigating these parameters on an atomic scale.[3-11] Pioneering studies by Heiz *et al*. have shown that the CO oxidation reaction rate over size-selected Pt_n clusters supported on MgO(100) is strongly influenced by the cluster size.[3] They also found that Au_n clusters on MgO(100) catalyse the CO oxidation at low temperature only in the presence of surface oxygen vacancies due to charging of the clusters.[4,5] Kaden *et al*. reported a study of CO oxidation over $Pd_n/TiO_2(110)$, where both CO adsorption and CO_2 production varied non-monotonically with size and the activity was shown to correlate with Pd core level shifts.[6,7] Vadja *et al*. found that Pt_n (n = 8-10) clusters stabilized on high-surface-area supports are 40-100 times more active for the oxidative dehydrogenation of propane than previously studied Pt and vanadia catalysts, where quantum chemical calculations indicate that under-coordination of the Pt atoms in the clusters is responsible for the surprisingly high reactivity compared with extended surfaces.[8] Mao *et al* investigated Pd_n (n = 4, 10, and 17) clusters on Al_2O_3 supports under oxidizing and reducing conditions, and found that the Pd atoms in direct contact with Al_2O_3 differ in oxidation state from the surface Pd atoms in a foil under reaction conditions.[9] Watanabe *et al*. studied CO oxidation reactions over $Pt_n/TiO_2(110)$ in high pressure conditions and found that the activation energy is correlated strongly with the cluster structure.[10] Bonanni *et al*. reported that the CO oxidation reaction over

$Pt_7/TiO_2(110)$ shows high catalytic activity when the TiO_2 support is slightly reduced; however, a strongly reduced substrate quenches the reaction.[11] These studies clearly indicate that catalytic properties are largely influenced by the adsorption states of the clusters: oxidation states, structure, and shape of the clusters. In this study, we investigated the adsorption states of size-selected Pt_n clusters on an Al_2O_3 surface.

Pt clusters on an Al_2O_3 surface are of special interest because Pt and Al_2O_3 are important materials in conventional automotive exhaust catalysts. On the stoichiometric $Al_2O_3(0001)$ surface, the dominant adhesion mechanism of the Pt overlayer is principally ascribed to polarization effects.[12-18] However, experimental studies of the oxide surface are often hampered because it is difficult to use methods involving charged particles with almost perfect insulators. Ultra-thin oxide films that are thin enough to avoid charge accumulation represent an elegant solution to this problem. It has been shown that atomically flat 0.54-nm-thick crystalline layers of aluminium oxide can be obtained by the oxidation of a single-crystalline NiAl(110) surface.[19,20] This surface was confirmed to be distinct from the Al_2O_3 bulk phases, as demonstrated by the overall film stoichiometry of $Al_{10}O_{13}$.[20] Additionally, domain boundary (DB) networks are formed to release misfit-induced lattice strain in the film.[21-25]

For ultra-thin films, the substrate metal–oxide interaction may interfere with the intrinsic behavior of the oxide material.[26-30] This interplay usually causes the emergence of new film-specific properties. Therefore, the use of thin oxide films grown on metal substrates is not only advantageous for exploring oxide materials themselves, but it also opens up the possibility of fabricating a new class of tunable compounds.[26,29] As demonstrated for the interaction of Au with Al_2O_3/NiAl(110), the attachment of a single Au atom induces the cleavage of an Al–O bond in the film, leading to the

formation of a new Al–Au bond.[31,32] Consequently, the Au atom becomes negatively charged owing to electron transfer from the NiAl substrate.[31,32] On the other hand, charge-induced adsorption mechanism is not active for Pd atoms and clusters on Al_2O_3/NiAl(110).[33-35] Pt deposits on Al_2O_3/NiAl(110) have been studied using several techniques.[36-40] Vapor deposited Pt atoms form single-layer islands randomly distributed on the surface,[36] where low-energy electron-diffraction spots of the oxide are strongly attenuated by the Pt deposits.[37] At one-monolayer coverage, the Pt 4*f* level was observed to be at a higher binding energy than that of bulk Pt.[38] CO molecules adsorb at ontop site of Pt deposits and dissociative adsorption was also observed.[38,39] Recently, we reported on a study of size-selected Pt_7 deposition on an Al_2O_3/NiAl(110) surface, where Pt_7 clusters were thermally immobile at 300 K and transiently migrated in a soft-landing process; these Pt clusters prefered to bind to DBs with planar structures.[40]

In this work, we combine scanning tunneling microscopy (STM), infrared reflection absorption spectroscopy (IRAS), and temperature-programmed desorption (TPD) to investigate the adsorption states of size-selected Pt_n clusters on Al_2O_3/NiAl(110). STM is one of the most powerful tools because of its atomic-scale resolution. It has been used in several studies to reveal the structures of deposited clusters.[31-33,41-45] Additionally, CO can be used as a probe molecule because its adsorption is known to be sensitive to structural and electronic peculiarities of the local environment.[4,30,46-50] Thus, chemical states of Pt atoms inside the size-selected clusters were probed by CO adsorption using IRAS and TPD. The experimental results presented here provide insight into the interrelation between the structure of size-selected Pt_n clusters and the chemical state of Pt atoms inside the clusters.

2. Experimental

Experiments were performed in an ultrahigh vacuum chamber (<1 × 10^{-8} Pa).[51] The thin aluminium oxide film grown on the NiAl(110) substrate was used for STM, IRAS and TPD experiments. The NiAl(110) substrate was 10 mm in diameter and oriented to within 0.1° (Surface Preparation Laboratory) for the STM experiments, and was 6 × 10 mm in size oriented to within 0.5° (Metal Crystals & Oxides Ltd.) for the IRAS and TPD experiments. For IRAS and TPD experiments, the temperature was monitored by a chromel-alumel (*K*-type) thermocouple that was spot-welded to the side of the substrate. The clean NiAl(110) surface was prepared by several cycles of Ar ion sputtering, followed by annealing at 1300 K. The thin aluminium oxide film was prepared by dosing 1800 L (Langmuir: 1 × 10^{-6} Torr s) of oxygen at 600 K, followed by annealing at 1100 K for 5 min.[19] The process was repeated several times in order to close open metal patches in the film.

Pt cluster ions were produced by a dc magnetron sputtering cluster source.[51] Size-selected Pt_n cluster ions were deposited on Al_2O_3/NiAl(110) from the surface normal at 300 K. The impact energy was tuned to <2 eV/atom (average impact energy was <1 eV/atom) by adjusting the bias voltage applied to the surface (soft-landing condition). The total amount of Pt deposited, determined from the integrated Pt_n^+ neutralization current on the sample, was 0.7–1.0 × 10^{13} atoms for STM and 5 × 10^{13} atoms for the IRAS and TPD experiments (in a deposition area with a diameter of ~5 mm). Due to an intensity distribution of the cluster ion beam, number density of deposited clusters depends on analysis position in STM experiments.

STM measurements were performed at 78 K using a low-temperature STM (LT-STM, Omicron GmbH) with a Nanonis (SPECS Zurich GmbH) or SCALA (Omicron GmbH) controller and a tungsten tip. The STM images were taken at a positive sample bias (V_s) of 3.5 V and a tunneling current (I_t) of 0.1 nA.

IRAS measurements were performed using a Fourier-transform infrared spectrometer (Bruker IFS66v/S) with a mercury–cadmium–telluride detector. The incident beam was passed through a KRS-5 polarizer to remove the unwanted s-polarized component. All the spectra were taken at 4 cm^{-1} resolution over 200 scans. IRAS spectra were recorded at a sample temperature of 88 K.

In the TPD measurements, desorbing molecules were detected by a quadrupole mass spectrometer (QMS, Pfeiffer, PrismaPlus QMG220M1). The ionization region was enclosed in a small glass envelope (Feulner cup),[52] and the crystal surface was placed in front of a small opening (3 mm diameter) in this cup at a distance of 1 mm.

^{13}CO (Cambridge Isotope Laboratories, isotopic purity 99%) gas was introduced through a pulse gas dosing system onto the sample surface. Exposure was estimated by comparing the CO coverage uptake on Ni(111) with that previously reported.[53]

3. Results and Discussion

Figures 1(a–d) show STM topographic images of Pt_n (n = 7, 13, 17, 19) clusters deposited on Al_2O_3/NiAl(110). The Al_2O_3 surface is terminated by oxygen atoms.[19,20] The Al_2O_3 film grows in two reflection domains (A, B) tilted by ±24° with

respect to the [1$\bar{1}$0] direction of NiAl(110).[19] In Fig. 1(a), the upper and lower terraces of the film are domains A and B, respectively. The bright stripes are DBs, which appear as line defects of the oxide film.[21-25] Reflection (between domains A and B) and anti-phase DBs (between A-A and B-B) are the main structural defects in the film. The topographic contrast of the DBs arose not from the height difference but from the electronic effect: the structure is atomically flat across the DBs.[21-25] Observed protrusions, located both inside the Al_2O_3 domains and on the DBs, were assigned to size-selected Pt_n clusters. In this study, the area fraction of the DBs was estimated to be 10 ± 2% of the Al_2O_3 surface, where the width of the DBs was assumed to be 1.8 nm based on STM line profiles. However, 26 ± 7% of the deposited Pt_n clusters were observed on the DBs, irrespective of the cluster size (n = 7–20). This result indicates the transient migration of the clusters because Pt_n clusters were thermally immobile at 300 K. [40]

The morphology of the Pt_n clusters was investigated by analyzing the apparent height of the Pt_n clusters. Figure 2 shows the apparent height of the Pt_n clusters on Al_2O_3/NiAl(110) as a function of cluster size. Figures 2(a) and 2(b) are histograms of Pt_n clusters adsorbed inside the Al_2O_3 domains and on the DBs, respectively. The average apparent height is shown in Figs. 2(c) (inside the Al_2O_3 domains) and 2(d) (on the DBs). By comparing Figs. 2(a) and 2(b) [or 2(c) and 2(d)], it is apparent that the Pt_n clusters adsorbed inside the Al_2O_3 domains and on the DBs show similar size dependence of their apparent height. At $n \leq 18$, the average apparent height is ~0.40 nm and almost size independent, but the apparent height abruptly increases to ~0.53 nm at n = 19. Because Pt_7 clusters lay flat on the Al_2O_3 surface with a planar structure,[40] the morphology of the Pt_n clusters ($n \leq 18$) could be assigned to a two-dimensional (2D)

planar structure and that of $n \geq 19$ to a three-dimensional (3D) two-layered structure. Note that the distribution of apparent height is relatively broad, which would be due to the intrinsic structural inhomogeneity of the oxide film.[20] The surface of the Al_2O_3 film is relatively inhomogeneous,[20] so that a number of different Pt_n adsorption configurations are possible.

The above assignments are supported by considering the apparent height of the Al_2O_3 film. As described in the introduction, the Al_2O_3 film on NiAl(110) is an atomically flat 0.54-nm-thick layer.[19,20] Hansen *et al*. reported that the apparent height of the Al_2O_3 film shows a clear bias-dependence in the V_s range between +1 and +4 V due to the electronic band gap of the Al_2O_3 film.[54] In this experimental conditions of V_s = 3.5 V and I_t = 0.1 nA, the apparent film height was estimated to be 0.30 nm by measuring the height difference between the bare and the oxide-covered areas (not shown). Thus, the apparent film height differs 0.24 nm from the structure of the Al_2O_3 film (0.54 nm). Assuming that the tip height above the film and that above the cluster are the same, cluster height may be estimated by subtracting 0.24 nm from the measured apparent cluster height. Note that this estimation may be too simplified because metal-induced unoccupied states were observed in the band gap of the Al_2O_3 film by the presence of Pt clusters.[40] However, the average cluster height at $n \leq 18$ and $n \geq 19$ was estimated to be 0.16 nm (= 0.40 – 0.24) and 0.29 nm (= 0.53 – 0.24), respectively, which are reasonable for 2D planar and 3D two-layered structures.

The energy balance of Pt–oxide and Pt–Pt bonds controls the morphology of Pt_n clusters on the Al_2O_3/NiAl(110) surface.[55] The adsorption energy of Pt_n clusters on the oxide would be written as $E_{2D(3D)} = N_{Pt\text{-}Ox}E_{Pt\text{-}Ox} + N_{Pt\text{-}Pt}E_{Pt\text{-}Pt}$, where $E_{2D(3D)}$ is the adsorption energy of 2D planar (3D two-layer) Pt_n clusters, $N_{Pt\text{-}Ox(Pt\text{-}Pt)}$ is the number of

Pt atom–oxide (Pt–Pt) bonds in a single cluster, and $E_{Pt\text{-}Ox(Pt\text{-}Pt)}$ is the single bond energy between a Pt atom and the oxide (Pt and Pt). Assuming that $N_{Pt\text{-}Ox}$ is equal the number of first layer Pt atoms in direct contact with the surface, and $E_{Pt\text{-}Ox}$ and $E_{Pt\text{-}Pt}$ equal the adsorption energy of a single Pt atom on the Al_2O_3 surface [recent density functional theory (DFT) studies calculated the adsorption energy to be ~2 eV for a Pt atom on the bulk Al_2O_3 surface[15,17,18]] and the single bond energy in the bulk Pt (one-sixth of the cohesive energy: 5.86/6 ~ 1 eV/bond), respectively, the size dependence of $N_{Pt\text{-}Ox}$ and $N_{Pt\text{-}Pt}$ controls the adsorption energies. In this simple model, E_{2D} and E_{3D} of Pt_4 were calculated using ($N_{Pt\text{-}Ox}$, $N_{Pt\text{-}Pt}$) = (4, 5) for the 2D cluster and ($N_{Pt\text{-}Ox}$, $N_{Pt\text{-}Pt}$) = (3, 6) for the 3D cluster, respectively (model structures are shown in Fig. 3). Figure 3 shows the energy difference between E_{2D} and E_{3D} as a function of cluster size, in which close packing is considered. A negative value means that the 3D two-layer structure is preferred to the 2D planar structure. Interestingly, the morphological preference changes from 2D to 3D at approximately n = 15~20, which is in reasonable agreement with our STM results. This model is simplistic because $E_{Pt\text{-}Ox(Pt\text{-}Pt)}$ would have size dependence and it also depends on the adsorption sites. However, it is interesting that the present simple model agrees reasonably well with the STM result.

Based on DFT calculations of free Pt clusters, it has been reported that planar clusters of up to nine atoms are more stable than their 3D isomers.[56-58] In this study, it was revealed that Pt_n clusters at $n \leq 18$ adsorb as a 2D planar structures on the Al_2O_3/NiAl(110) surface. Previously, preferential 2D growth of metal deposits on thin oxide films was observed, i. e., charge-mediated adsorption mechanisms.[26-30,32] Au clusters interact with the Al_2O_3/NiAl(110) substrate via charge transfer from the metal substrate and Coulomb interactions in combination with polaronic distortions of the

oxide substrate.[31,32] Similar charge-mediated adsorption mechanisms should be considered in order to understand the adsorption mechanism of Pt clusters on Al_2O_3/NiAl(110) because the electronegativity of Pt (2.28) is comparable with that of Au (2.54).

In order to shed light on the adsorption mechanism, we investigated CO adsorption on Pt_n/Al_2O_3/NiAl(110) using IRAS. Adsorption of CO probe molecules and the measurement of their vibrational properties are often employed to identify the oxidation state of metal atoms or nanoparticles grown on oxide surfaces.[4,30,46-50] Figure 4(a)–(c) shows IRAS spectra of ^{13}CO adsorbed on Pt_n/Al_2O_3/NiAl(110) (n = 7, 15, 20) as a function of CO exposure. CO adsorption and IRAS measurements were performed at 88 K. Because CO molecules could not adsorb on the Al_2O_3/NiAl(110) surface at 88 K,[59] the observed IRAS peaks were assigned to CO molecules bound to the Pt_n clusters. At the initial stage of CO adsorption on the Pt_7 cluster, Fig. 4(a), a broad peak is observed at ~2010 cm^{-1}. With increasing exposure, the high-frequency peak at 2040 cm^{-1} grows in intensity, and the intensity saturates with a low-frequency shoulder at 0.30 L. On Pt_{15}/Al_2O_3/NiAl(110), Fig. 4(b), an IRAS peak is observed at 2000 cm^{-1} at 0.05 L. With increasing exposure, the peak shifts to 2020 cm^{-1}; a shoulder peak at ~2040 cm^{-1} is also observed. On Pt_{20}/Al_2O_3/NiAl(110), two peaks at 2045 and 2005 cm^{-1} are clearly observed at 0.05 L. With increasing exposure, the peak at 2005 cm^{-1} grows in intensity, accompanied by a blue shift to 2020 cm^{-1}, which then dominates the IRAS intensity at saturation coverage. The observed peak shifts (2000–2020 cm^{-1}) would be due to intermolecular interactions such as dipole–dipole coupling.[46,60] It should be mentioned that it needs very small CO exposure for saturated adsorption on Pt_n clusters, indicating that a reverse spillover mechanism dominates CO attachment to Pt_n

clusters.[1,61] For equal nominal coverage of the Pt atoms, the capture zone is sensitively dependent on the cluster size.[1,61] However, saturated adsorption was reached at about the same exposure of ~0.3 L (Fig. 4). In this experimental condition, lateral distance between the Pt_n clusters would be several nm. Because adsorption energy of CO on the Al_2O_3/NiAl(110) surface is 0.14~0.17 eV,[59] CO molecules would be trapped for >1μs before desorption at 88 K. Using the translational velocity of two-dimensional ^{13}CO gas at 88 K (~200 m/s), incoming CO molecules travel >1μm on the surface which largely exceeds the lateral distance between the Pt_n clusters. Therefore, saturated adsorption was reached at about the same exposure irrespective of the cluster size.

Previous studies have reported that the vibrational frequency of adsorbed CO on single-crystalline Pt surfaces is 2060–2010 cm^{-1} at an ontop site and 1840–1810 cm^{-1} at a bridge site.[62,63] On the Pt oxide ($Pt^{+/2+}$), CO molecules were observed at ≥2080 cm^{-1}.[64] Recently, the vibrational frequencies of a single ontop CO molecule adsorbed on gas-phase cationic/neutral/anionic $Pt_n^{+/0/-}$ clusters were reported: 2070–2020 cm^{-1} on Pt_n^+, 2010–1960 cm^{-1} on Pt_n^0, and 1955–1820 cm^{-1} on Pt_n^-, respectively (isotopically shifted from reported values).[65] As described above, because of the high electronegativity of Pt, negative charging of Pt_n clusters would be expected on the Al_2O_3/NiAl(110) surface, as reported for Au clusters.[31,32] However, the observed peak positions indicate that CO molecules were adsorbed at ontop site of neutral and/or slightly cationic Pt atoms. It should be mentioned that if CO molecules were adsorbed on anionic Pt atoms with their molecular axis parallel to the surface, they could not be detected by IRAS because of the surface selection rule. However, because only a single desorption peak was observed in TPD (discussed below), we exclude anionic Pt atoms in the Pt_n clusters adsorbed on the Al_2O_3/NiAl(110) surface.

The observed IRAS peaks are broad as compared with those found in single crystalline studies,[62,63] which would be due to the structural inhomogeneity of Pt_n clusters as deduced from the apparent height distribution. However, adsorbed CO seems to be composed of two ontop species: high- (HF_{CO}: 2045–2040 cm^{-1}) and low- (LF_{CO}: 2020–2000 cm^{-1}) frequency peaks. The frequency difference between HF_{CO} and LF_{CO} is ~40 cm^{-1} at low coverage. Two peaks are clearly visible by comparing the IRAS spectra at saturation CO coverage, as shown in Fig. 4(d) (see gray dashed curves). With increasing cluster size, the intensity of the HF_{CO} decreases, whereas that of the LF_{CO} increases. As described above, the fraction of Pt_n clusters bound to the DBs is independent of cluster size. Thus, the observed size dependence of the IRAS spectra should be explained not by the adsorption sites of Pt_n clusters on Al_2O_3/NiAl(110) (inside the domains or on the DBs) but on the chemical environment of Pt atoms in individual clusters. The size dependence of the IRAS peak intensities indicates that the HF_{CO} and LF_{CO} are associated with the first-layer and second-layer Pt atoms, respectively.

The LF_{CO} (2020–2000 cm^{-1}) is compatible in frequency with ontop CO adsorbed at step sites of the bulk Pt surfaces (2030–2015 cm^{-1}),[62,66-68] indicating that this ontop species adsorbs on coordinatively unsaturated Pt atoms in the clusters. The IRAS peak intensity of Pt_{20} is dominated by LF_{CO}. Based on the STM result that Pt_{20} is a two-layer 3D structure, it would be reasonable to assign LF_{CO} to Pt atoms that are bound mainly by Pt–Pt bond in the cluster. HF_{CO} is blue shifted by ~40 cm^{-1} from LF_{CO} at low coverage. On the bulk Pt surface, the vibrational frequency of the CO stretch mode is ~20 cm^{-1} higher on terrace sites than on step sites,[62,66-68] and so the coordination number of Pt atoms would be insufficient to explain the observed blue shift. It is well

known that a stretching vibrational frequency of adsorbed CO shifts to a higher frequency when it is co-adsorbed with an electronegative species such as oxygen.[69-71] Theoretical studies have shown that electronegative atoms have a strong influence on the nearest-neighbour metal surface atoms but a weaker influence on other metal atoms.[72,73] In the case of metal clusters on an oxide surface, metal atoms would interact with the oxygen atoms of the oxide surface. Thus, the observed HF_{CO} (2045–2040 cm^{-1}) may be ascribed to Pt atoms interacting with the oxygen atoms of the Al_2O_3 surface. This assignment was corroborated with a co-adsorption experiment of O_2 and CO on the Pt_n clusters. In Fig. 4(d), the black curves show co-adsorbed ^{13}CO with ^{18}O, where the Pt_n/Al_2O_3/NiAl(110) surface was exposed to 500 L $^{18}O_2$ at 300 K (in order to dissociate O_2 molecules), followed by CO adsorption at 88 K. Interestingly, only HF_{CO} was observed, irrespective of cluster sizes. This result supports the above assignment that HF_{CO} is related to Pt atoms interacting with substrate oxygen atoms.

With increasing cluster size, as shown in Fig. 4(b) (gray dashed curve), HF_{CO} decreases in intensity and LF_{CO} increases. Therefore, the fraction between the two kinds of Pt atoms in the cluster depends on the cluster size. Based on the results, it may be said that the number of adsorption and/or reaction sites depends on the cluster size, which may contribute to the size-dependent chemical reactivity of Pt_n clusters on the Al_2O_3 surface.

Several DFT calculations have been reported for Pt deposits on bulk Al_2O_3 surfaces. On an α-Al_2O_3 surface, it was reported that Pt atoms transfer electrons to the surface oxygen atoms and form an ionic bond,[13,16] which is consistent with the results seen with Al_2O_3 films on Al(111).[14] In contrast, other studies have reported that the bonding mechanism involves charge rearrangement on Pt and covalent Pt–O

bonding.[15,17] With increasing coverage, the adsorption mechanism of the Pt monolayer to the Al_2O_3 surface is dominated by the polarization effect.[13,14] On the other hand, on γ-Al_2O_3, it was reported that the Al_2O_3 surface transfers ~0.2–0.3 electrons to the Pt atom.[18] In this study, two kinds of Pt atoms are identified inside the cluster by means of IRAS, LF_{CO} and HF_{CO}, which are assigned as coordinatively unsaturated neutral Pt atoms and slightly cationic Pt atoms interacting with substrate oxygen, respectively. Rigorous charge of Pt_n clusters would be determined by comparing the IRAS peak positions and DFT calculations as previously performed for Au/MgO(100).[4,30,48-50]

Finally, it is informative to investigate the adsorption strength of CO to Pt_n clusters. Figure 5 shows ^{13}CO TPD spectra adsorbed on Pt_n/Al_2O_3/NiAl(110), where the Pt_n clusters were saturated by CO at 88 K followed by TPD measurement. The amount of Pt deposits was 5×10^{13} atoms and the heating rate was 3.5 K/s. Note that, in this experiment, QMS sensitivity was not calibrated, and so the intensity of each spectrum was normalized to allow for a simple line shape comparison. The bottom spectrum was measured after the Al_2O_3/NiAl(110) was exposed to 0.5 L CO at 88 K. As reported previously, CO does not adsorb on the surface at 88 K.[59] When the Pt_7 clusters were deposited, only single CO desorption was observed at 495 K. The asymmetric peak shape indicates first-order desorption. On Pt_{15} and Pt_{20}, similar desorption peaks were observed at ~500 K. Note that other desorption peaks were not observed up to 1000 K (not shown). After the first TPD experiments up to 1000 K, adsorbed CO was not observed using IRAS by exposing the surface to CO at 88 K (not shown). This result indicates that the amount of Pt decreased by the 1000 K heating, which is consistent with the previous report that the Pt atoms diffuse into the oxide at ≥560 K.[36] Using the redhead analysis with first-order desorption and a pre-exponential factor of 10^{13} s^{-1}, the

desorption activation energy of CO from Pt_n (n = 7, 15, 20) was estimated to be ~1.3 eV, which is nearly the same value as that the step sites on the Pt surfaces.[68] In the IRAS experiments, two ontop CO species were observed; however, only a single TPD peak was observed, which may be due to a small adsorption energy difference between HF_{CO} and LF_{CO}. Note that CO_2 and O_2 desorption were not observed (not shown), and thus adsorbed CO molecules did not react with the oxide substrate.

When sub-monolayer Pt was vapor deposited at 100 K on Al_2O_3/NiAl(110), a CO desorption peak was also observed at ~500 K.[38] On the other hand, when the Pt was deposited at 300 K, two desorption peaks were observed at ~150 and ~500 K with comparable intensities and CO dissociation took place.[38] Thus, Pt deposits on which CO dissociation takes place would be characterized by the 150 K desorption peak. In our case, only the 500 K peak was observed, therefore CO molecules molecularly adsorb and desorb on the Pt_n/Al_2O_3/NiAl(110) surface. Note that vapor-deposited Pt particles (diameter ~1.7 nm) on the bulk α-Al_2O_3 surface also show a single CO desorption peak at ~500 K.[74]

By taking our results into account, we gain insight about the interrelation between the structure of size-selected Pt_n clusters and the chemical state of Pt atoms inside the clusters as follows. Pt_n clusters were adsorbed as 2D planar structures at $n \leq$ 18 on the Al_2O_3 surface. By using CO probe molecules, it was determined that the Pt_7 cluster is predominantly composed of slightly cationic Pt atoms due to the interaction between Pt atoms and substrate oxygen atoms. With increasing cluster size, the number of neutral Pt atoms, bound in the cluster by lateral Pt–Pt bonds increases. Above n = 19, Pt_n clusters are adsorbed as 3D two-layer clusters, and the adsorption sites of CO are dominated by the neutral Pt atoms. This size dependence of the Pt atoms inside the

cluster, that is, the size dependence of the numbe of adsorption/reaction sites, may contribute to the size-dependent chemical reactivity of Pt_n clusters on the Al_2O_3 surface.

Conclusions

The morphology and CO adsorption properties of size-selected Pt_n clusters ($7 \leq n \leq 20$) on Al_2O_3/NiAl(110) were investigated by STM, IRAS, and TPD. Pt_n clusters adsorbed flat on the surface with a planar structure at $n \leq 18$; 3D two-layer structures started to appear at $n = 19$. This morphological transition could be reasonably explained by a simple model in which the number of Pt–oxide and Pt–Pt bonds in the cluster is considered. CO molecules adsorbed at ontop site of the Pt_n clusters with an adsorption energy of ~1.3 eV. Two kinds of ontop CO species were observed by IRAS: HF_{CO} (2045–2040 cm^{-1}) and LF_{CO} (2020–2000 cm^{-1}). HF_{CO} and LF_{CO} were assigned as adsorbed CO on slightly cationic Pt atoms interacting with substrate oxygen atoms and on neutral Pt atoms bound by Pt–Pt bond inside the clusters, respectively. Based on the assignments, the chemical states of the Pt atoms inside the clusters were discussed. Pt_7 clusters were predominantly composed of slightly cationic Pt atoms, but the number of neutral Pt atoms increased with increasing cluster size. For 3D clusters, the adsorption sites of CO were dominated by the neutral Pt atoms. This size dependence of the Pt atoms inside the cluster may contribute to the size-dependent chemical reactivity of Pt_n clusters on the Al_2O_3 surface.

Notes and references

[a] *Toyota Central R&D Labs., Inc., 41-1 Yokomichi, Nagakute, Aichi 480-1192, JAPAN*

[b] *Toyota Motor Corporation, 1200 Mishuku, Susono, Shizuoka 410-1193, JAPAN*

** Corresponding author: Tel: +81–561–71–7950;*

E-mail: e0827@mosk.tytlabs.co.jp

1. U. Heiz and U. Landman, *Nanocatalysis*, Springer, 2007.

2. W. Harbich, in: K. M. Meiwes-Broer (Ed.). *Metal clusters at surfaces*, Springer, Berlin, 2000, p107.

3. U. Heiz, A. Sanchez, S. Abbet and W. -D. Schneider, *J. Am. Chem. Soc*., 1999, **121**, 3214.

4. B. Yoon, H. Häkkinen, U. Landman, A. S. Wörz, J. M. Antonietti, S. Abbet, K. Judai and U. Heiz, *Science*, 2005, **307**, 403.

5. A. Sanchez, S. Abbet, U. Heiz, W. –D. Schneider, H. H äkkinen, R. N. Barnett and U. Landman, *J. Phys. Chem. A*., 1999, **103**, 9573.

6. W. E. Kaden, T. Wu, W. A. Kunkel and S. L. Anderson, *Science*, 2009, **326**, 826.

7. W. E. Kaden, W. A. Kunkel, F. S. Roberts, M. Kane and S. L. Anderson, *J. Chem. Phys*., 2012, **136**, 204705.

8. S. Vajda, M. J. Pellin, J. P. Greeley, C. L. Marshall,L. A. Curtiss, G. A. Ballentine, J. W. Elam, S. Catillon-Mucherie, P. C. Redfern, F. Mehmood and P. Zapol, *Nature Materials*, 2009, **8**, 213.

9. B. -H. Mao, R. Chang, S. Lee, S. Axnanda, E. Crumlin, M. E. Grass, S. -D. Wang, S. Vajda and Z. Liu, *J. Chem. Phys*., 2013, **138**, 214304.

10. Y. Watanabe, X. Wu, H. Hirata and N. Isomura, *Catal. Sci. Technol*., 2011, **1**, 1490.

11. S. Bonanni, K. Aït-Mansour, W. Harbich and H. Brune, *J. Am. Chem. Soc*., 2012, **134**, 3445.

12. Q. Fu and T. Wagner, *Surf. Sci. Rep*., 2007, **62**, 431.

13. C. Verdozzi, D. R. Jennison, P. A. Schultz and M. P. Sears. *Phys. Rev. Lett*., 1999, **82**, 799.

14. A. Bogicevic and D. R. Jennison, *Phys. Rev. Lett*., 1999, **82**, 4050.

15. B. Hinnemann and E. A. Carter, *J. Phys. Chem. C*. 2007, **111**, 7105.

16. C. Zhou, J. Wu, T. J. D. Kumar, N. Balakrishnan, R. C. Forrey and H. Cheng, *J. Phys. Chem. C*., 2007, **111**, 13786.

17. L. G. Briquet, C. R. A. Catlow and S. A. French, *J. Phys. Chem. C*., 2008, **112**, 18948.

18. N. A. Deskins, D. M.ei and M. Dupuis, *Surf. Sci*., 2009, **603**, 2793.

19. R. Jaeger, H. Kuhlenbeck, H. -J. Freund, M. Wutting, W. Hoffmann, R. Franchy and H. Ibach, *Surf. Sci*., 1991, **259**, 235.

20. G. Kresse, M. Schmid, E. Napetschnig, M. Shishkin, L. Köhler and P. Varga, *Science*, 2005, **308**,

1440.

21. M. Kulawik, N. Nillus, H. -P. Rust and H. -J. Freund, *Phys. Rev. Lett*., 2003, **91**, 256101.

22. G. H. Simon, T. Köning, H. -P. Rust, M. Heyde and H. -J. Freund, *New J. Phys*., 2009, **11**, 093009.

23. G. H. Simon, T. Köning, L. Heinke, L. Lichtenstein, M. Heyde and H. -J. Freund, *New J. Phys*., 2011, **13**, 123028.

24. M. Schmid, M. Shishkin, G. Kresse, E. Napetschnig, P. Varga, M. Kulawik, N. Nillus, H. -P. Rust and H.-J. Freund, *Phys. Rev. Lett*., 2006, **97**, 046101.

25. N. Nillus, M. Kulawik, H. -P. Rust and H.-J. Freund, *Phys. Rev. B*., 2004, **69**, 121401(R).

26. N. Nillus, *Surf. Sci. Rep*., 2009, **64**, 595.

27. D. Ricci, A. Bongiorno, G. Pacchioni and U. Landman, *Phys. Rev. Lett*., 2006, **97**, 036106.

28. M. Sterre, T. Risse, M. Heyde, H. -P. Rust and H.-J. Freund, *Phys. Rev. Lett*., 2007, **98**, 206103.

29. H. -J. Freund and G. Pacchioni, *Chem. Soc. Rev*., 2008, **37**, 2224.

30. H.-J. Freund, *Oxide Ultrathin Films: Science and Technology*, G. Pacchioni, S. Valeri (Eds.), Wiley-VCH Verlag Weinheim, 2012, p145.

31. N. Nillus, V. G. Pirovano, V. Bradzova, M. Kulawik, J. Sauer and H. -J. Freund, *Phys. Rev. Lett*., 2008, **100**, 096802.

32. N. Nillus, V. G. Pirovano, V. Bradzova, M. Kulawik, J. Sauer and H. -J. Freund, *Phys. Rev. B*, 2010, **81**, 045422.

33. N. Nillus, T. M. Wallis and W. Ho, *Phys. Rev. Lett*., 2003, **90**, 046808.

34. R. Robles and S. N. Khanna, *Phys. Rev. B*., 2010, **82**, 085428.

35. T. Wu. W. E. Kaden, W. A. Kunkel and S. L. Anderson, *Surf. Sci*., 2009, **603**, 2764.

36. T. Bertrams, F. Winkelmann, Th. Uttich, H. –J. Freund and H. Neddermeyer, *Surf. Sci*., 1995, **331-333**, 1515.

37. J. Libuda, M. Bäumer and H. -J. Freund, *J. Vac. Sci. Technol. A*., 1994, **12**, 2259.

38. S. Wohlrab, F. Winkelmann, J. Libuda, M. Bäumer, H. Kuhlenbeck, H. -J. Freund, in: R. J. MacDonald, E. C. Taglauer, and K. R. Wandelt (Eds.), *Surface science: Principles and current applications*, Springer, Berlin 1996, p193.

39. H.-J. Freund, B. Dillmann, D. Ehrlich, M. Hassel, R.M. Jaeger, H. Kuhlenbeck, C.A. Ventrice Jr., F. Winkelmann, S. Wohlrab, C. Xu, Th. Bertrams, A. Brodde and H. Neddermeyer, *J. Mol. Catal*., 1993, **82**, 143.

40. A. Beniya, N. Isomura, H. Hirata and Y. Watanabe, *Chem. Phys. Lett*., 2013, **576**, 49.

41. A. Piednoir, E. Perrot, S. Granjeaud, A. Humbert, C. Chapon and C. R. Henry, *Surf. Sci*., 1997, **391**, 19.

42. H. Jödicke, R. Schaub, R. Monot, J. Buttet and W. Harbich, *Surf. Sci*., 2001, **475**, 109.

43. R. Schaub, H. Jödicke, F. Brunet, R. Monot, J. Buttet and W. Harbich, *Phys. Rev. Lett*., 2001, **86**,

3590.

44. H. Yasumatsu, T. Hayakawa and T. Kondow, *J. Chem. Phys*., 2006, **124**, 014701.

45. N. Isomura, X. Wu and Y. Watanabe, *J. Chem. Phys*. 2009, **131**, 164707.

46. F. M. Hoffmann, *Surf. Sci. Rep*., 1983, **3**, 107.

47. M. Frank, M. Bäumer, R. Kühnemuth and H. -J. Freund. *J. Phys. Chem. B*., 2001, **105**, 8569.

48. M. Sterrer, M. Yulikov, E. Fischbach, M. Heyde, H.-P. Rust, N. Nilius, G. Pacchioni, Th. Risse and H.-J. Freund. *Angew. Chem. Int. Ed*., 2006, **45**, 2630.

49. M. Sterrer, Th. Risse, M. Yulikov, H.-J. Freund, J. Carrasco, F. Illas, C. Di Valentin, L. Giordano and G. Pacchioni. *Angew. Chem. Int. Ed*., 2006, **45**, 2633.

50. X. Lin, B. Yang, H.-M. Benia, P. Myrach, M. Yulikov, A. Aumer, M.A. Brown, M. Sterrer, O. Bondarchuk, E. Kieseritzky, J. Rocker, T. Risse, H.-J. Gao, N. Nilius and H.-J. Freund, *J. Am. Chem. Soc*., 2010, **132**, 7745.

51. Y. Watanabe and N. Isomura, *J. Vac. Sci. Technol. A*., 2009, **27**, 1153.

52. J.T. Yates, Jr., *Experimental Innovations in Surface Science: A Guide to Practical Laboratory Methods and Instruments*, Springer-Verlag, New York, 1998.

53. A. Beniya, N. Isomura, H. Hirata, Y. Watanabe, *Surf. Sci*., 2012, **606**, 1830.

54. K. H. Hansen, T. Worren, E. Lægsgaard, F. Besenbacher and I. Stensgaard, *Surf. Sci*., 2001, **475**, 96.

55. C. T. Campbell, *Surf. Sci. Rep*., 1997, **27**, 1.

56. L. Xiao and L. Wang, *J. Phys. Chem. A*., 2004, **108**, 8605.

57. K. Bhattacharyya and C. Majumder, *Chem. Phys. Lett*., 2007, **446**, 374.

58. V. Kumar and Y. Kawazoe, *Phys. Rev. B*., 2008, **77**, 205418.

59. R.M. Jaeger, J. Libuda, M. Bäumer, K. Homann, H. Kuhlenbeck and H.-J. Freund, *J. Electron Spectrosc. Relat. Phenom*., 1993, **64/65**, 217.

60. F. Vanolli, U. Heiz and W. -D. Schneider, *Chem. Phys. Lett*. 1997, **277**, 527.

61. M. A. Röttgen, S. Abbet, K. Judai, J. -M. Antonietti, A. S. Wörz, M. Arenz, C. R. Henry and U. Heiz, *J. Am. Chem. Soc*., 2007, **129**, 9635.

62. R. K. Brandt, R. S. Sorbello and R. G. Greenler, *Surf. Sci*., 1992, **271**, 605.

63. B. E. Hayden and A. M. Bradshaw, *Surf. Sci*., 1983, **125**, 787.

64. A.A. Davydov, *Infrared Spectroscopy of Adsorbed Species on the Structure of Transition Metal Oxides*, John Wiley & Sons, Chichester, 1990.

65. P. Gruene, A. Fielicke, G. Meijer and D. M. Rayner, *Phys. Chem. Chem. Phys*., 2008, **10**, 6144.

66. B. E. Hayden, K. Kretzshemar, A. M. Bradshaw and R. G. Greenler, *Surf. Sci*., 1985, **149**, 394.

67. J. Yoshinobu, N. Tsukahara, F. Yasui, K. Mukai and Y. Yamashita, *Phys. Rev. Lett*., 2003, **90**, 248301.

68. J. Xu, P. N. Henriksen and J. T. Yates, Jr., *Langmuir*, 1994, **10**, 3663.

69. M. Trenary, K. J. Uram and J. T. Yates, Jr., *Surf. Sci.*, 1985, **145**, 512.

70. Z. Xu, L. Surnev, K. J. Uram and J. T. Yates, Jr., *Surf. Sci*., 1993, **292**, 235.

71. J. Yoshinobu and M. Kawai, *J. Chem. Phys*., 1995, **103**, 3220.

72. P. J. Feibelman and D. R. Hamann, *Phys. Rev. Lett*. 1984, **52**, 61.

73. J. M. Maclaren, J. B. Pendry, R. W. Joyner and P. Meehan, *Surf. Sci*., 1986, **175**, 263.

74. E. I. Altman and R. J. Gorte, *Surf. Sci*. 1988, **195**, 392.

Figure captions

Fig. 1. STM topographic images of $Pt_n/Al_2O_3/NiAl(110)$ (V_s = 3.5 V, I_t = 0.1 nA, 50 × 50 nm): (a) n = 7, (b) n = 13, (c) n = 17, and (d) n = 19. Pt_n clusters were deposited at 300 K, followed by STM measurements at 78 K.

Fig. 2. Size dependence of apparent height of Pt_n clusters on $Al_2O_3/NiAl(110)$. Histgrams of the apparent height of Pt_n clusters adsorbed (a) inside the Al_2O_3 domains and (b) on the DBs, respectively. Average apparent height of Pt_n clusters adsorbed (c) inside the Al_2O_3 domains, and (d) on DBs, respectively, where error bars represent the standard deviation. STM measurements were performed with V_s = 3.5 V and I_t = 0.1 nA at 78 K.

Fig. 3. Calculated energy difference of Pt_n clusters between 2D planar (E_{2D}) and 3D two-layer (E_{3D}) structures as a function of cluster size (see text). Schematics represent structural models of 2D and 3D clusters, where first- and second-layer Pt atoms are colored by gray and dark gray, respectively.

Fig. 4. IRAS spectra of ^{13}CO adsorbed on $Pt_n/Al_2O_3/NiAl(110)$ as a function of CO exposure: (a) n = 7, (b) n = 15, and (c) n = 20. Pt_n clusters (5×10^{13} atoms) were deposited at 300 K, followed by CO adsorption and IRAS measurements at 88 K. (d) IRAS spectra of adsorbed ^{13}CO at saturation coverage as a function of cluster size (gray dashed curve) for the same spectra shown in (a)–(c). The black solid curve represents the IRAS spectra of ^{13}CO co-adsorbed with O on $Pt_n/Al_2O_3/NiAl(110)$. Pt_n clusters (5 ×

10^{13} atoms) were deposited at 300 K, followed by $^{18}O_2$ exposure (500 L) at 300 K. ^{13}CO adsorption and IRAS measurements were performed at 88 K.

Fig. 5. TPD spectra of ^{13}CO adsorbed on $Pt_n/Al_2O_3/NiAl(110)$ at saturation ^{13}CO coverage as a function of cluster size (n = 7, 15, 20). Pt_n clusters (5×10^{13} atoms) were deposited at 300 K, followed by CO adsorption at 88 K. The bottom spectrum was measured after the $Al_2O_3/NiAl(110)$ surface was exposed to 0.5 L ^{13}CO at 88 K. The heating rate was set to 3.5 K/s. QMS sensitivity was not calibrated, and so the intensity of each spectrum was normalized to allow for a simple line shape comparison.

Figures

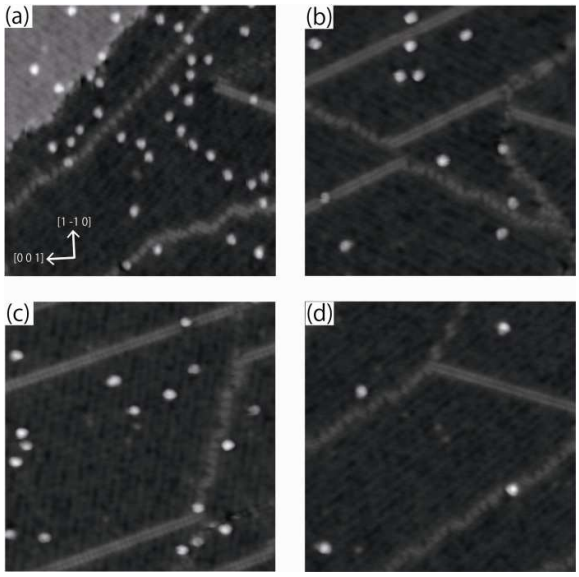

Fig. 1. Beniya et al.

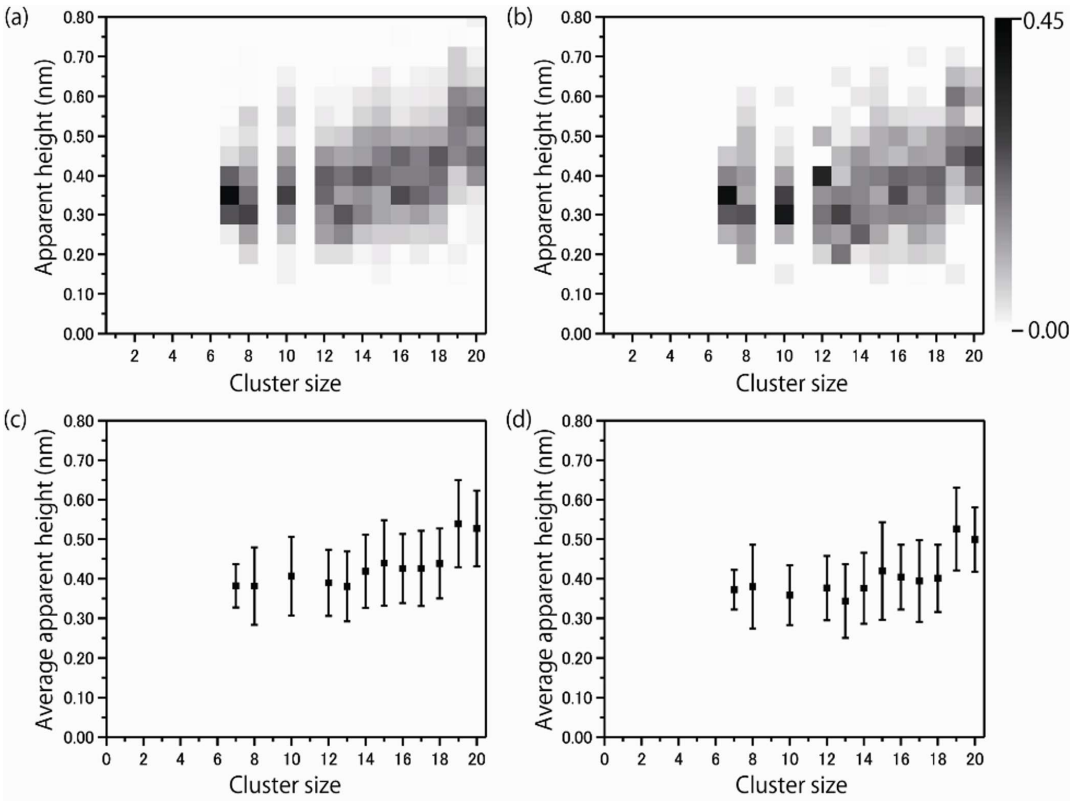

Fig. 2. Beniya et al.

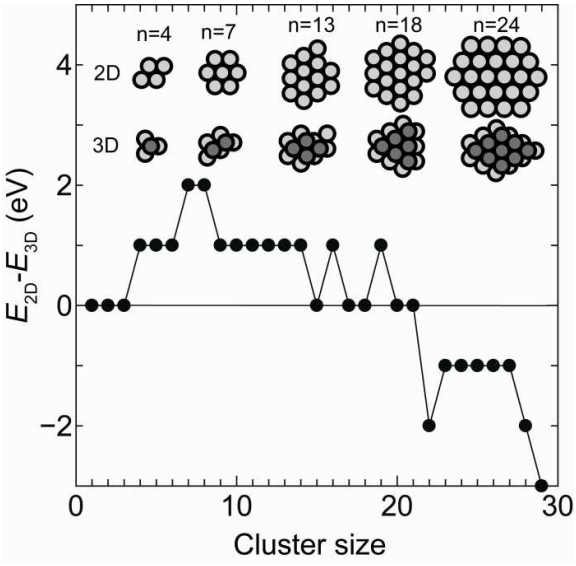

Fig. 3. Beniya et al.

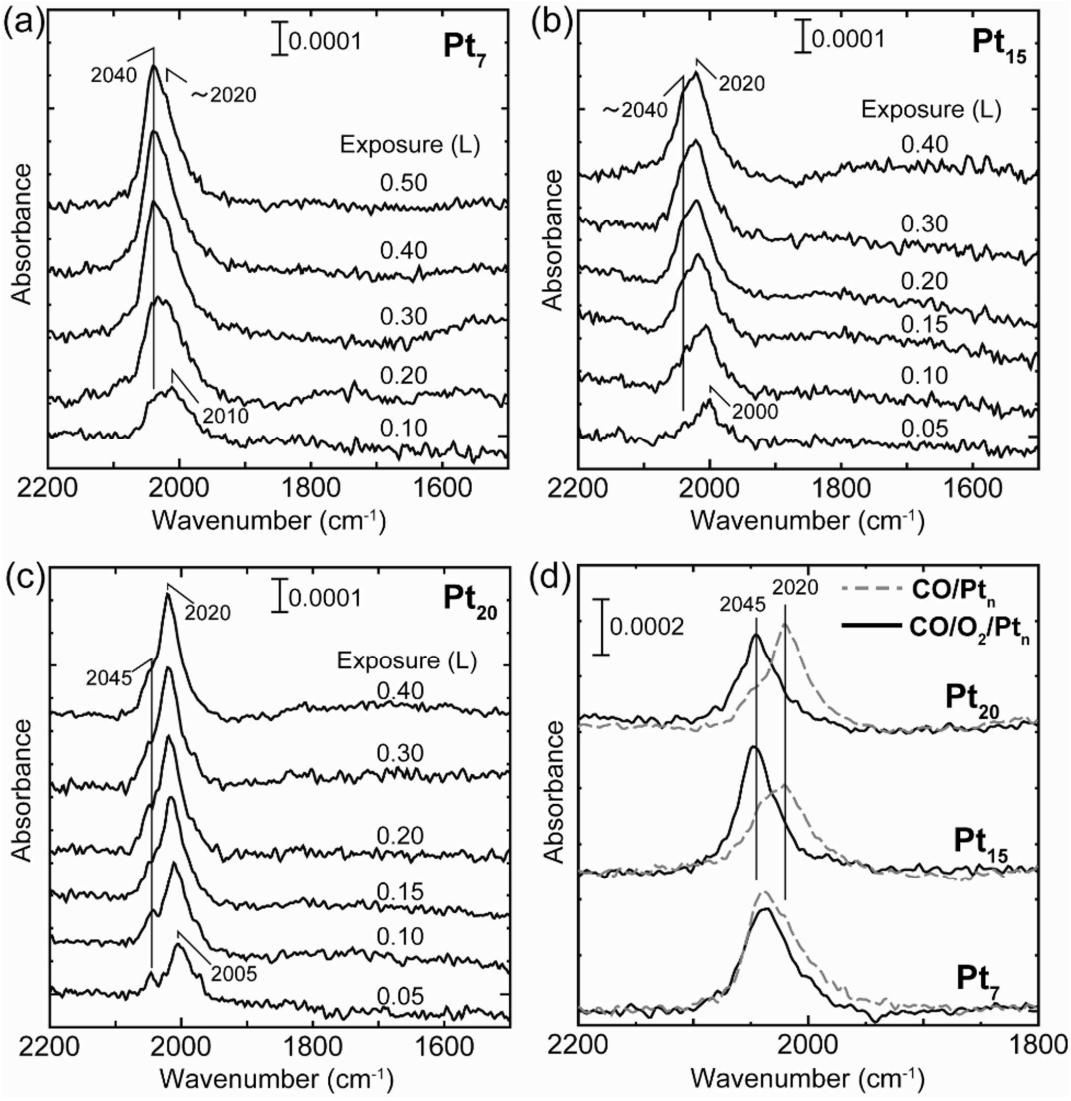

Fig. 4. Beniya et al.

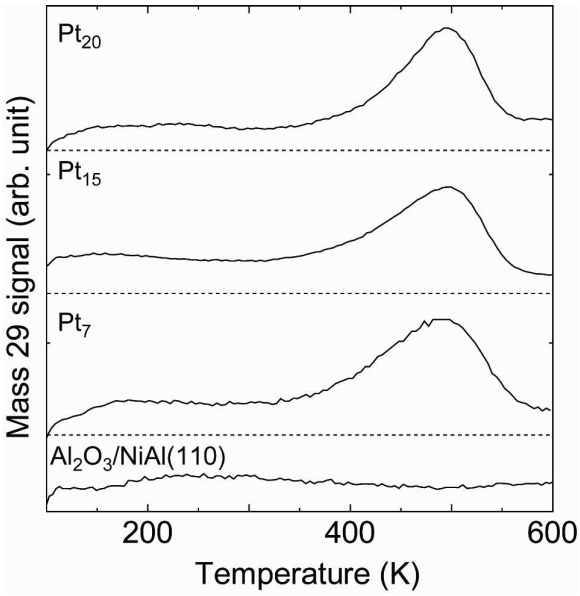

Fig. 5. Beniya et al.